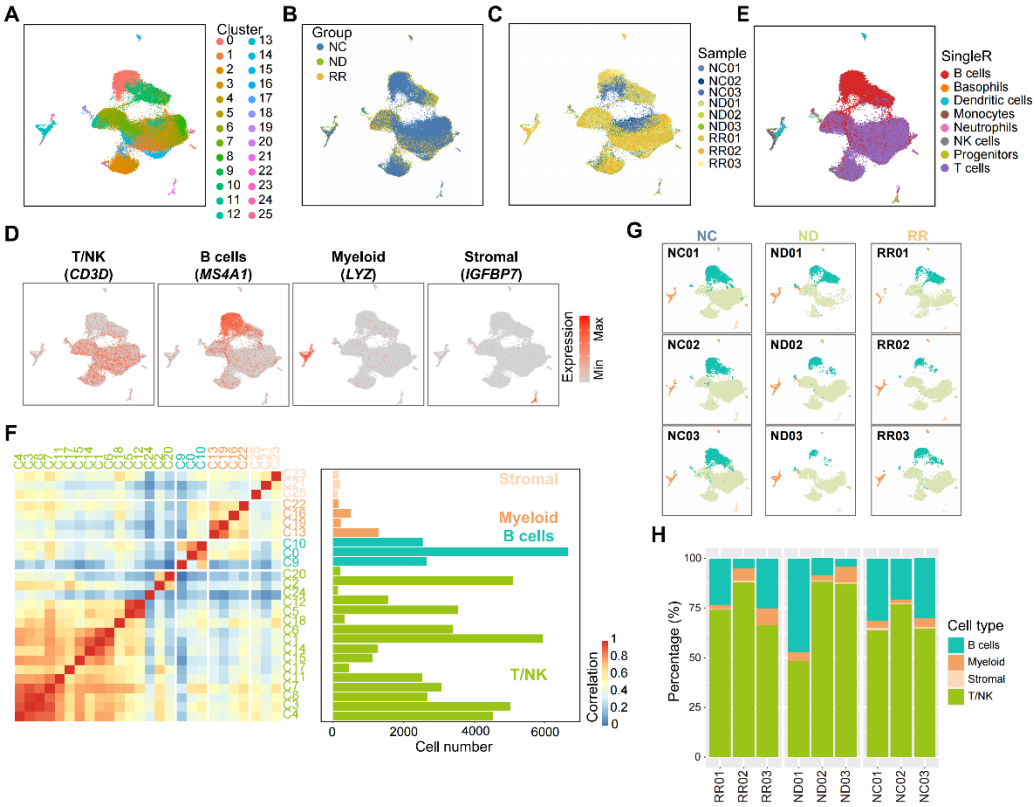


**Supplementary Figure 1. The cellular ecosystem of AITL characterized by scRNA-seq. (A)** Unsupervised clustering of 55482 cells illustrated in UMAP plot. **(B-C)** UMAP plots of all cells colored by groups(B) and samples(C). **(D)** UMAP plot showing the expression of representative markers of distinct cell types. **(E)** UMAP plot showing the cell type annotated by SingleR. **(F)** Hierarchical cluster analysis showing the correlation between the expression of the top 5 markers from distinct clusters with varying cell numbers. The bar plot illustrated the distribution of cell numbers in different clusters. **(G)** The cells from NC, ND-AITL and RR-AITL illustrated in UMAP plots, respectively. **(H)** Bar plot showed the percentage of distinct cell types within individual sample.

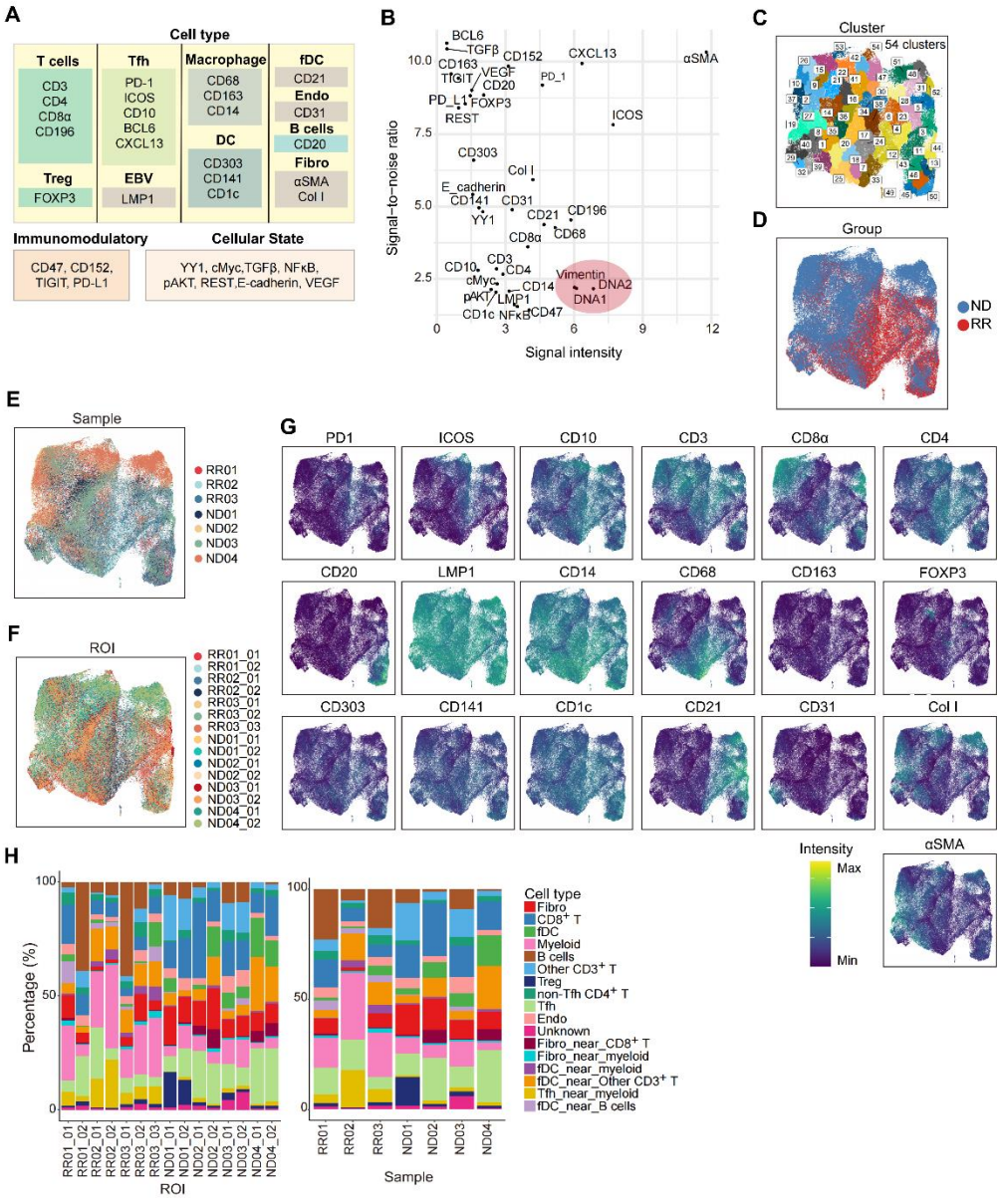


**Supplementary Figure 2. The cellular ecosystem of AITL characterized by IMC. (A)** The biomarker panel specifically designed for this research. These markers were categorized into three components: cell types, immunomodulatory, and cellular states. **(B)** Quality control for all markers used in IMC experiments. The x axis means signal intensity, the y axis means signal-to-noise ratio. The markers within the red circle were excluded. **(C-F)** UMAP plots of all cells colored by clusters (C), groups (D), samples (E) and ROIs (F). **(G)** Markers used for cell type identification illustrated in the UMAP plot. **(H)** Bar plots showing the cell type fractions within each ROI (left panel) and

sample (right panel).

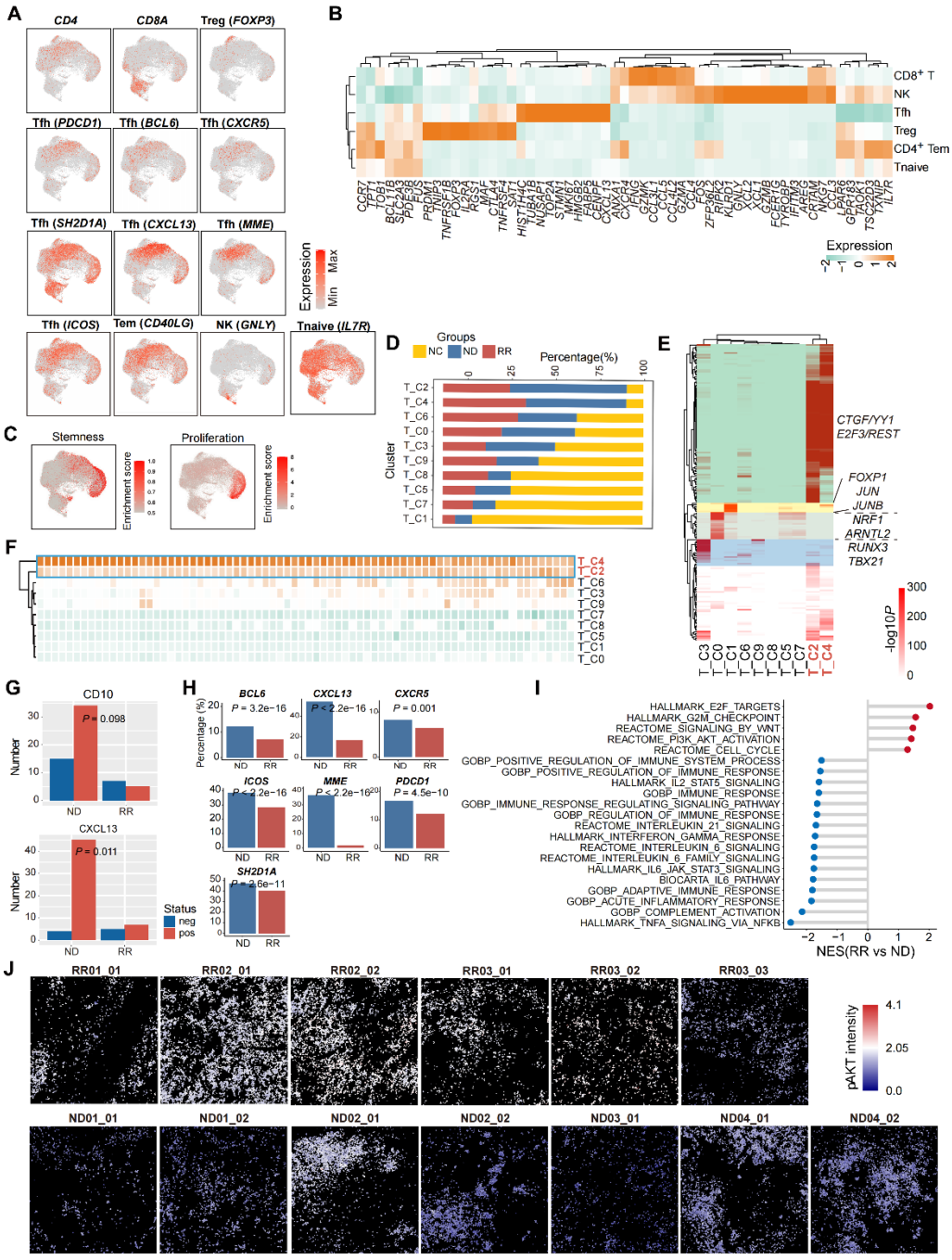


**Supplementary Figure 3. Unique features for malignant Tfh cells. (A)** The expression levels of canonical markers for T cell subtypes are depicted in the UMAP plots. **(B)** Heatmap showing representative marker expression of different T/NK subtypes. **(C)** The differentiation potential (left

panel) calculated by CytoTRACE and proliferation capacity (right panel) of T cells. **(D)** Barplot showing the fraction of T/NK cells from NC (yellow), ND-AITL (blue) and RR-AITL (red) samples in each cluster. **(E)** The heatmap illustrated TFs that significantly activated across different T cell clusters. **(F)** Heatmap showing the mean enrichment score of metabolism pathways across various clusters. **(G)** The number of patients with positive and negative IHC staining, with CD10 on the top and CXCL13 on the bottom. **(H)** The expression percentage of known AITL markers in Tfh cells between the RR-AITL and ND-AITL groups. *P* values were determined by fisher's exact test. **(I)** The lollipop plot illustrates the normalized enrichment scores of significantly differential pathways between the RR-AITL (red) and ND-AITL (blue) groups. **(J)** The IMC images showing the intensities of pAKT within malignant Tfh cells. The colors represent protein activity levels, ranging from lower (blue) to higher (red).

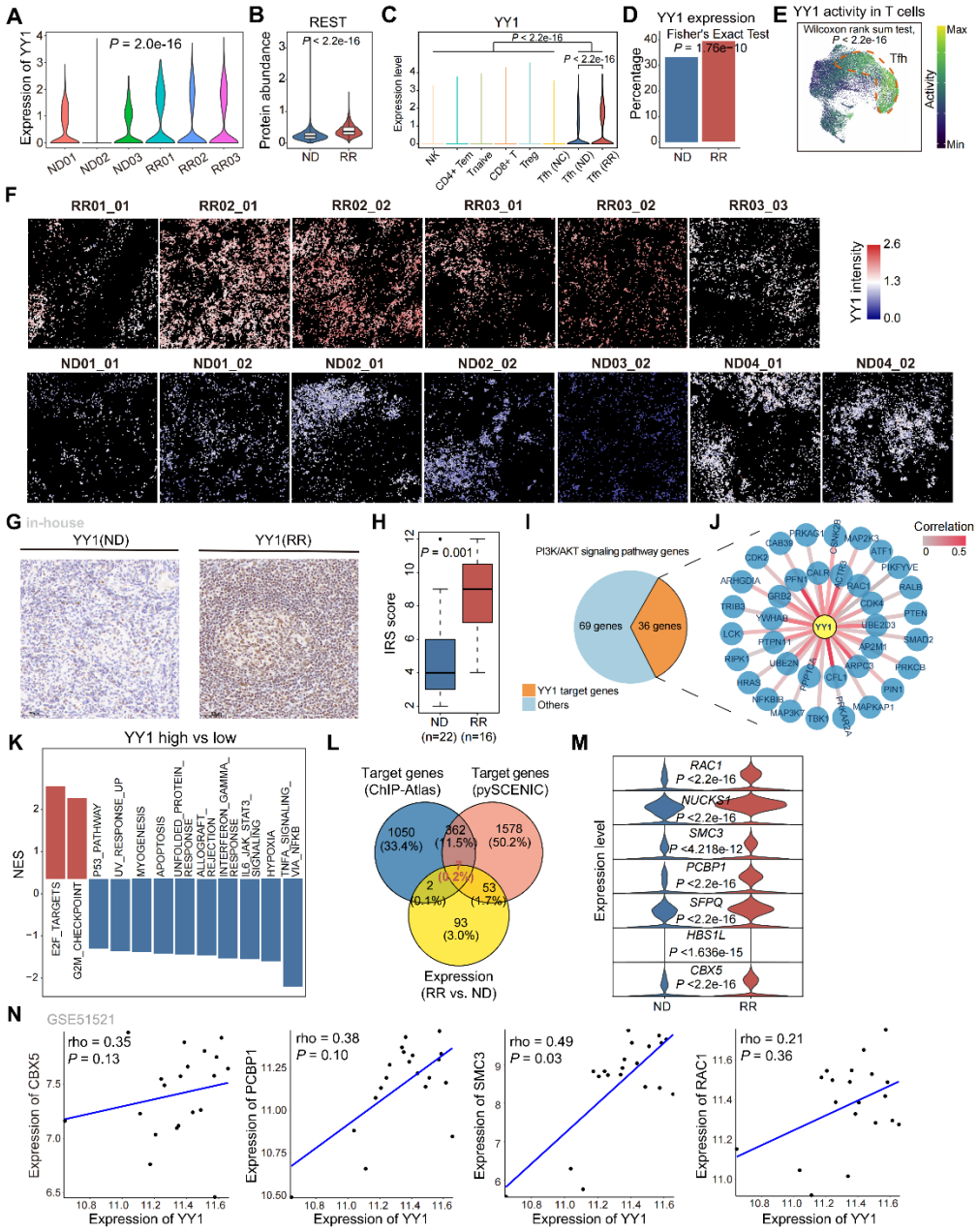


**Supplementary Figure 4. The underlying regulatory mechanism of YY1 promoting AITL progression. (A)** The expression of YY1 across various samples was depicted in a violin plot. **(B)** The intensities of REST in malignant Tfh cells. The *P* values were determined by two-sided unpaired Wilcoxon test. **(C)** Violin plot showing expression levels of YY1. *P* values were determined by two-sided unpaired Wilcoxon test. **(D)** Percentage of cells expressing YY1 across

Tfh from ND-AITL (blue) and RR-AITL (red). The *P* value was calculated using Fisher's exact test. **(E)** The UMAP plot demonstrates the transcriptional activity of YY1 in T cells. **(F)** The protein activity of YY1 within malignant Tfh cells shown on IMC images. The colors represent protein activity levels, ranging from lower (blue) to higher (red). **(G)** The IHC of YY1 in ND-AITL (left) and RR-AITL (right), respectively. **(H)** Boxplot illustrating the IRS scores differentiating between the RR-AITL and ND-AITL groups. **(I)** Pie chart showing the gene distribution within PI3K/AKT/mTOR signaling pathway. **(J)** Network illustrated the spearman correlation between TF YY1 and 36 target genes from (I). Color represents the correlation levels. **(K)** The significantly enriched hallmarks between malignant Tfh cells with higher YY1 activity to those with lower YY1 activity. The cells were stratified into two groups based on the median of YY1 activity. The normalized enrichment scores were calculated through GSEA analysis. **(L)** Venn plot illustrated the intersection of YY1 target genes identified from ChIP-Atlas, pySCENIC, and genes highly expressed in malignant Tfh cells from RR-AITL compared to ND-AITL. **(M)** Violin plot illustrated the expression differences of intersection genes obtained from (L). **(N)** Spearman correlation between expression of YY1 to that of four target genes showed in (I).

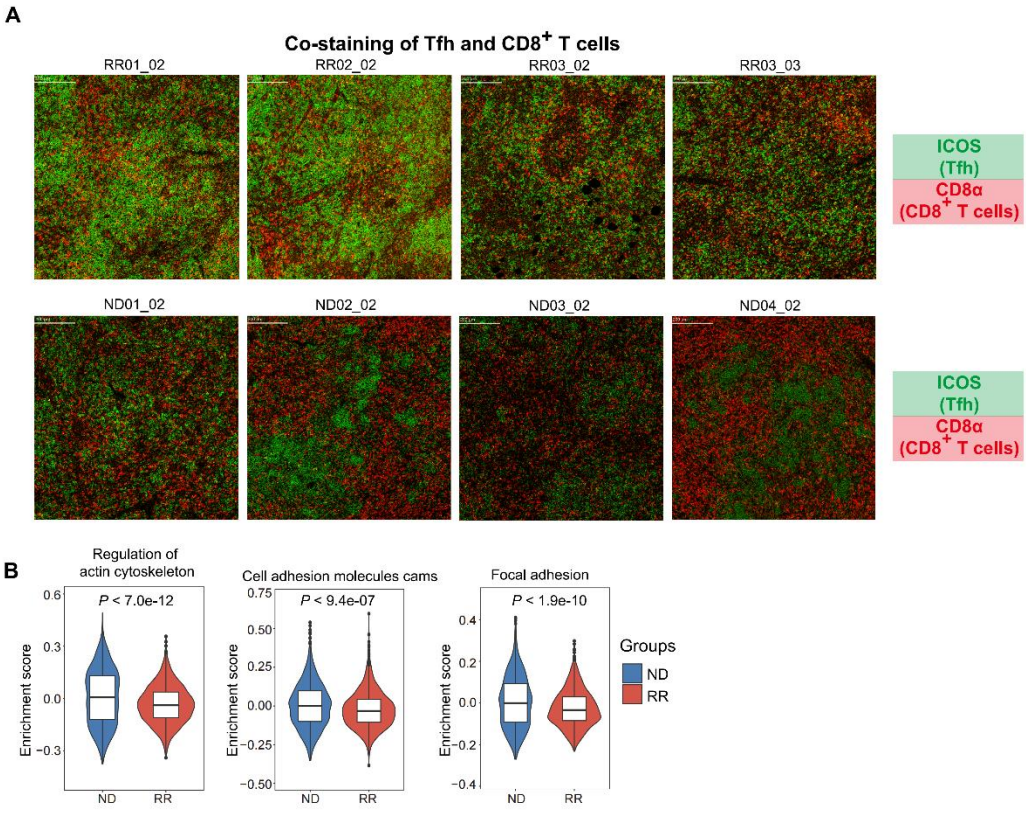


**Supplementary Figure 5. The co-staining of Tfh cells and CD8⁺ T cells. (A)** The representative markers for Tfh cells (ICOS; green) and CD8⁺ T cells (CD8α; red) stained in each ROI. **(B)** Enrichment scores of pathways related to T cell migration capacity in CD8⁺ T cells from ND-AITL and RR-AITL samples. *P* values were determined by two-sided unpaired Wilcoxon test.

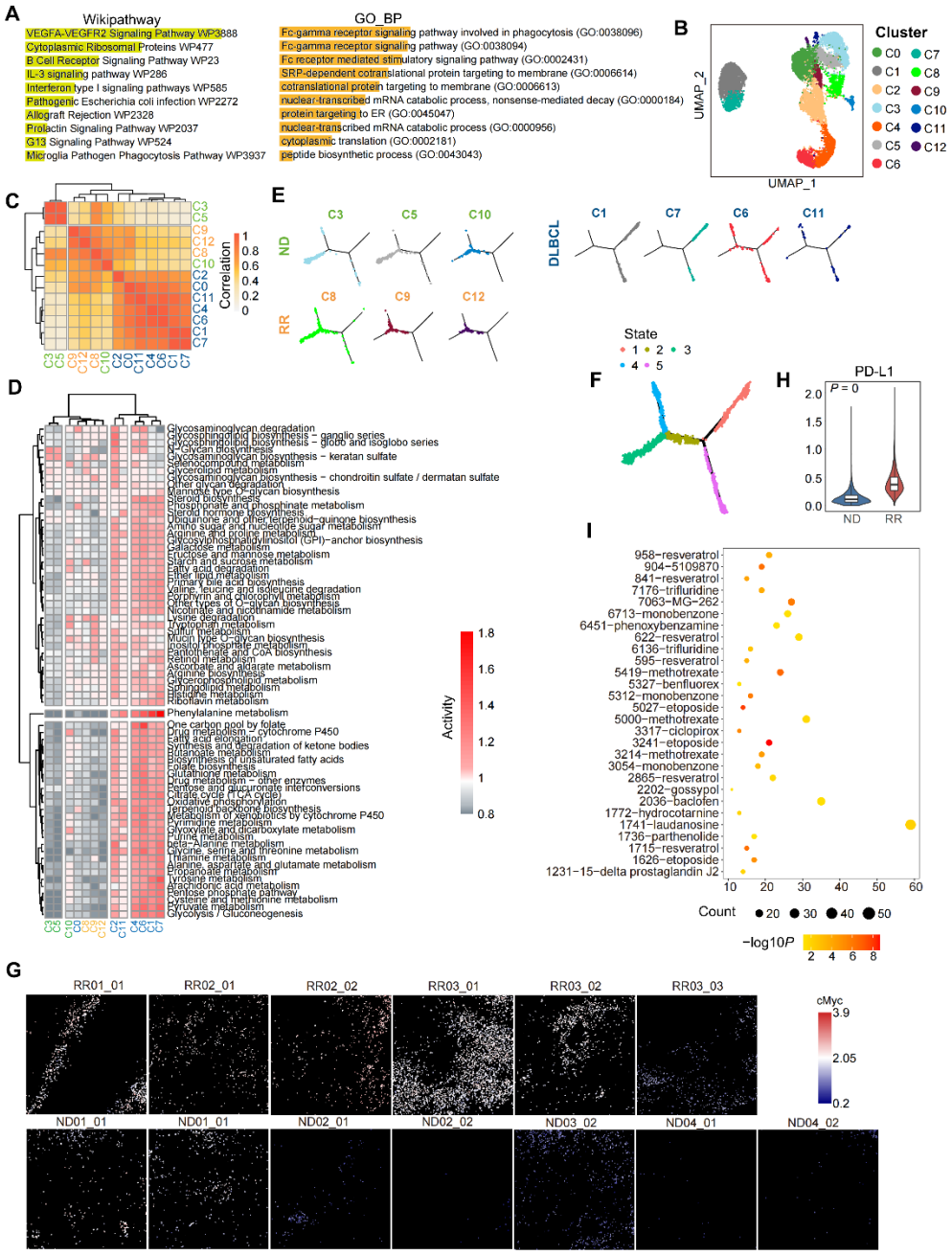


**Supplementary Figure 6. The characteristics of B cells in RR-AITL. (A)** The functional enrichment analysis for genes up-regulated in B cells from RR-AITL. **(B)** Unsupervised clustering of B cells from ND-AITL, RR-AITL and DLBCL samples. **(C)** Hierarchical cluster analysis showing the correlation of the expression levels of top 20 gene of each cluster. Different colored text represents ND-AITL (green), RR-AITL (orange) and DLBCL (blue) groups. **(D)** Heatmap

showing the activity of metabolic pathways across various B cell clusters. **(E)** The cells of each cluster are sorted by pseudotime along the trajectory. The different colored text represents ND-AITL, RR-AITL and DLBCL enriched clusters, respectively. **(F)** The trajectory plots showing the state of each cell. **(G)** The IMC images showing the protein activity of cMyc within B cells. The colors represent protein activity levels, ranging from lower (blue) to higher (red). **(H)** The protein levels of PD-L1 in B cells. *P* values were determined by two-sided unpaired Wilcoxon test. **(I)** Pharmacological agents predicted to impede malignant transformation of B cells. The color represents -log transformed *P* values. The size of the dots corresponds to the number of genes that intersect between the genes within modules two, three, and four identified through pseudotime analysis and the gene sets susceptible to down-regulation by these drugs.

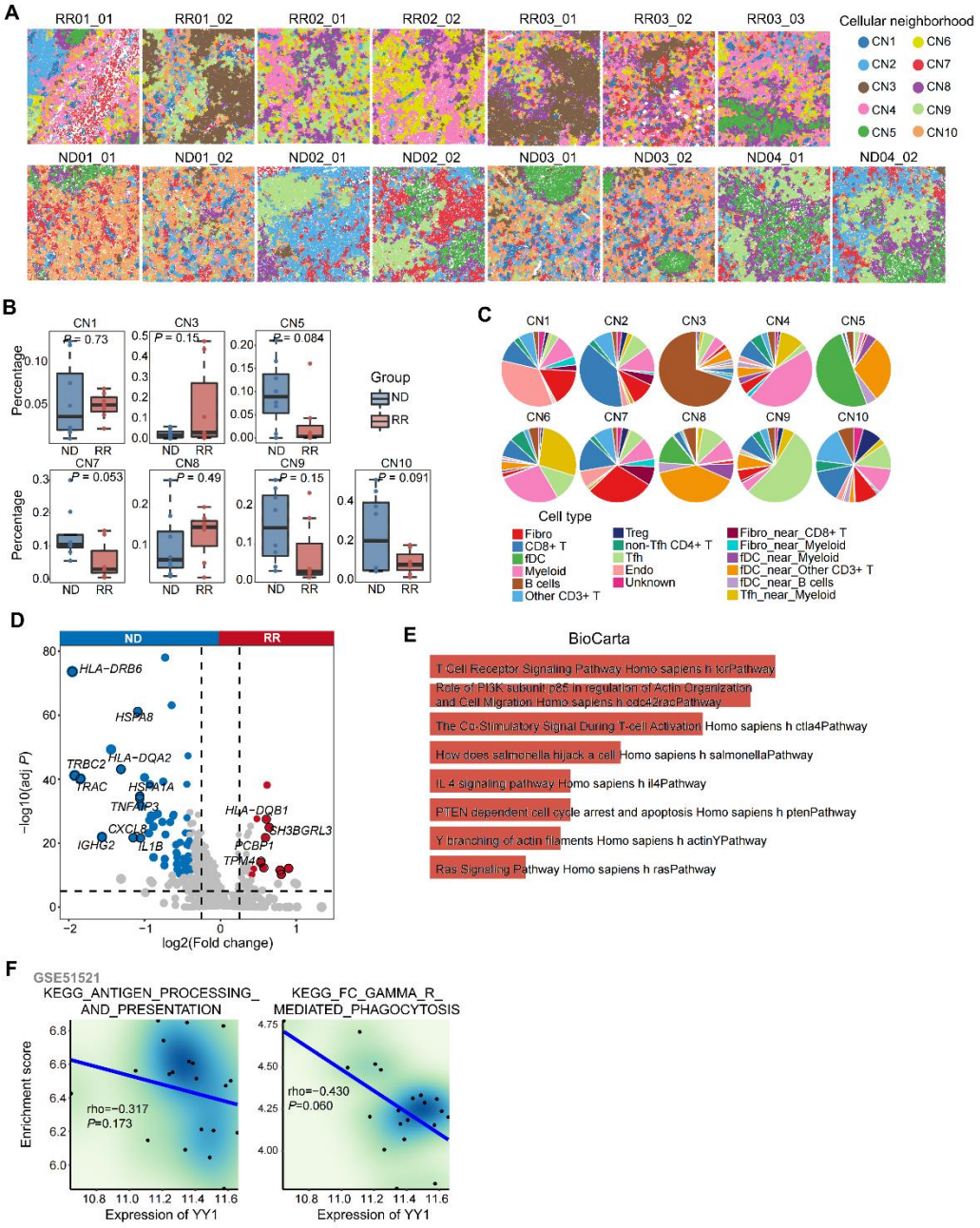


**Supplementary Figure 7. The difference of CNs between ND-AITL and RR-AITL. (A)** CNs shown in the images, the colors represent different CNs. **(B)** Box plot showing the percentage of CNs between RR-AITL and ND-AITL. *P* values were determined by two-sided unpaired Wilcoxon test. **(C)** Pie chart showing the cell type distribution within different CNs. **(D)** Volcano plot of expression changes between myeloid cells from ND-AITL and RR-AITL samples. Up-regulated

genes in RR-AITL (red) and ND-AITL (blue) are highlighted. **(E)** The enrichment analysis of up-regulated genes in myeloid cells from RR-AITL compared to ND-AITL. **(F)** The spearman correlation between YY1 expression and enrichment scores of antigen processing and presentation (left panel), phagocytosis (right panel) in GSE51521 dataset. Each data point represents individual sample.

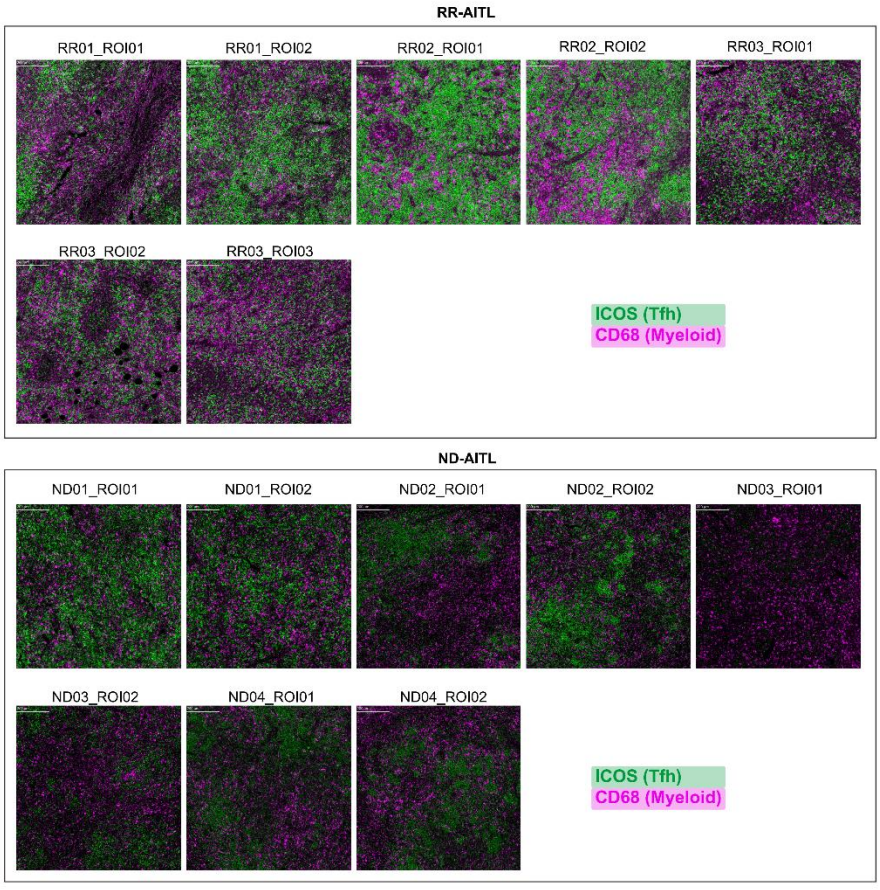


**Supplementary Figure 8. The co-staining of Tfh cells and myeloid cells.** The representative markers for Tfh cells (ICOS; green) and myeloid cells (CD68; purple) stained in each ROI.

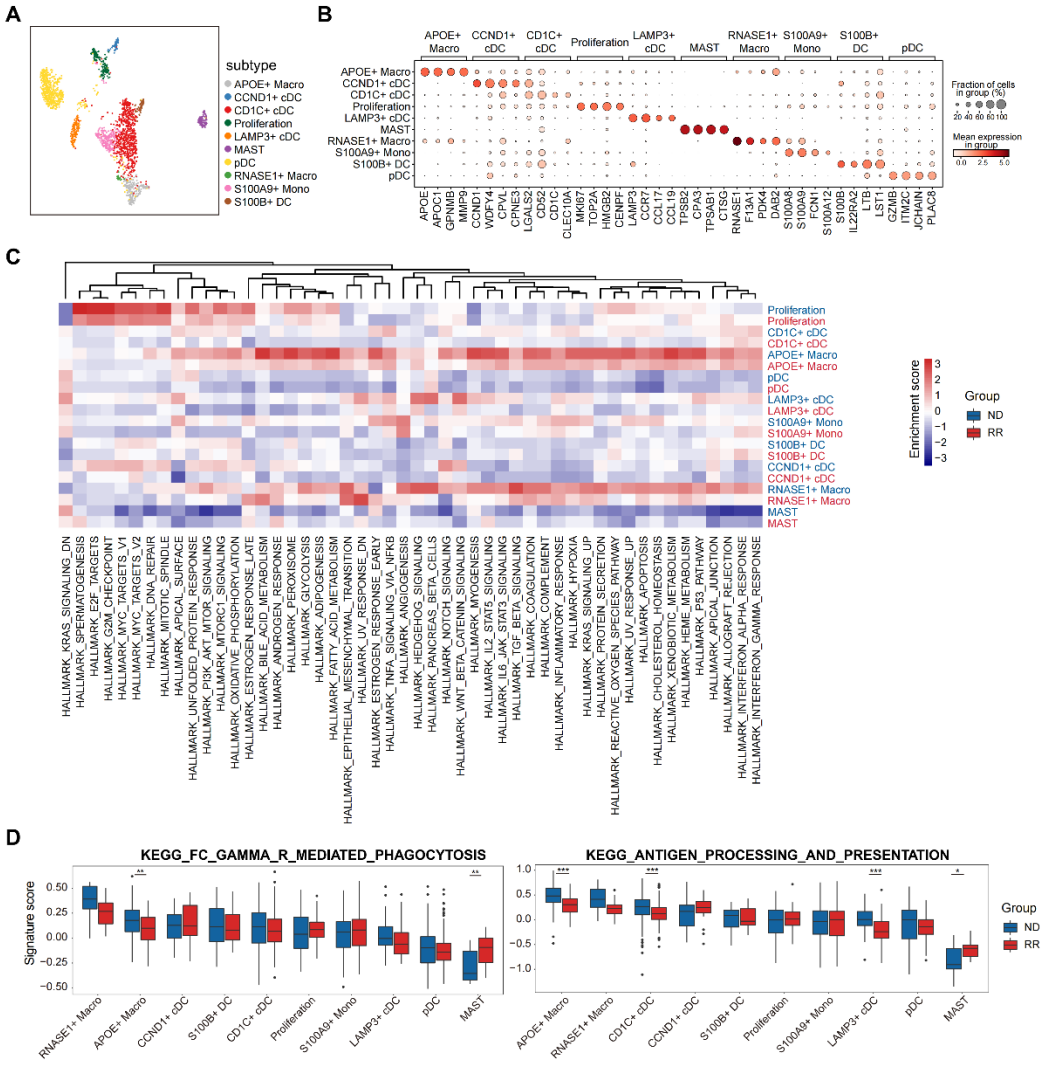


**Supplementary Figure 9. Analysis of functional changes in myeloid cell subtypes. (A)** Myeloid subtypes from NC, ND-AITL and RR-AITL illustrated in UMAP plots. **(B)** Dot plot depicting the expression of representative markers for myeloid subtypes. Dot size is indicative of the proportion of cells within each subtype expressing these markers, and dot color represents the mean expression levels of these markers within each subtype. **(C)** The heatmap displays the average hallmark enrichment scores for each subtype in the ND-AITL and RR-AITL samples. The color gradient from blue to red indicates scores ranging from low to high, while the labels are colored blue for ND-AITL and red for RR-AITL. **(D)** The violin plot depicts the pathway enrichment scores for each subtype

across the ND-AITL and RR-AITL samples. Statistical significance was assessed using a two-sided unpaired Wilcoxon test, with P values represented as follows: *, $P < 0.05$, **, $P < 0.01$, and ***, $P < 0.001$.